RNA interference suppression of Nogo-66 receptor prevents Nogo-66-mediated inhibition of invasion and adhesion and simultaneously increases cell apoptosis in C6 cells

SONG TONG[1], NANXIANG XIONG[1] and JIANYING SHEN[2]

[1]Department of Neurosurgery, Union Hospital, [2]Section of Histology and Embryology, Department of Anatomy, Tongji Medical College, Huazhong University of Science and Technology, Wuhan 430022, Hubei, P.R. China

Received July 15, 2013; Accepted August 5, 2013

DOI: 10.3892/or.2013.2694

Abstract. Gliomas are the most common primary tumors of the central nervous system (CNS). Nogo-66 is an extracellular domain of Nogo-A, which can block axon regeneration in the CNS after trauma. Some studies have indicated that Nogo-A and its receptor (NgR) are expressed in tumor tissues; however, their roles in tumors are still unknown. We report the impact of Nogo-66 and NgR on the proliferation, apoptosis, adhesion and invasion of C6 glioma cells. Short hairpin RNA (shRNA)-triggered RNA interference was used to inhibit NgR expression in C6 cells. Then, an *in vitro* cell adhesion assay was performed to assess the effect of NgR downregulation on the adhesion ability of C6 cells. In addition, a chamber assay and a cell scratch assay were conducted to test invasion ability. The spontaneous apoptosis of C6 cells was examined by flow cytometry, western blotting and terminal deoxynucleotidyl transferase dUTP nick end labeling (TUNEL) assay. NgR downregulation resulted in a significant increase of C6 adhesion and invasion activity in the presence of Nogo-66, markedly inhibited proliferation and induced spontaneous apoptosis. In conclusion, knockdown of NgR enhanced invasion and adhesion but increased cell apoptosis in C6 cells, suggesting that Nogo-66/NgR might have complex effects on glioma cells.

Introduction

Gliomas are the most common primary tumors that arise from glial cells, which still remain incurable despite treatments including surgical resection, radiotherapy and chemotherapy. They are considered to be highly invasive, metastatic and lacking apoptotic cell death. Thus, new treatment strategies for gliomas are urgently needed.

Nogo-A was first recognized as a myelin-associated neuronal growth inhibitor after spinal cord injury (1). Molecular cloning of Nogo-A led to the identification of a neuronal surface glycosylphosphatidylinositol (GPI)-linked receptor that binds to the 66 amino acid residue luminal/extracellular domain of Nogo-A (Nogo-66), termed the Nogo-66 receptor (NgR) (2). Nogo-66 and NgR have been mainly studied for their capabilities to block axon regeneration and neurite outgrowth. However, their functions in the normal central nervous system (CNS), especially in the developing CNS, are also receiving great interest.

In addition to their expression in oligodendrocytes and neurons, Nogo-A and NgR are detected in glioma cells (3,4). Although Nogo-A has been intensively studied for its inhibitory effect on axonal regeneration in the adult CNS, the functions of Nogo-A and NgR in tumors remain largely elusive. Liao *et al* have shown that substratum adherence and migration by human U87MG glioma cells in culture were significantly attenuated by the extracellular domains of Nogo-66 and myelin-associated glycoprotein (MAG) (3). U87MG cells contain large amounts of endogenous NgR and treatment of these cells with NgR antibodies results in an increase in their ability to adhere to, or migrate through, Nogo-66- and MAG-coated substrates. Therefore, Nogo-66 and MAG may modulate glioma growth and migration by acting through NgR.

Kilic *et al* suggest that supression of Nogo-A led to a decrease in neuronal survival, but the association between downregulation of NgR and tumor apoptosis remain unexplored (5).

In the present study, by using an RNA interference method with C6 cells, NgR expression was downregulated and the effects of NgR knockdown on tumor apoptosis, migration and cell adhesion *in vitro* were investigated. The results implied potentially important roles for Nogo-66 and NgR in the prevention of tumor invasion and metastasis as well as in the promotion of tumor apoptosis.

Materials and methods

Cell lines and culture conditions. Rat C6 glioma cells were cultured in Dulbecco's modified Eagle's medium (DMEM)

Correspondence to: Dr Nanxiang Xiong, Department of Neurosurgery, Union Hospital, Tongji Medical College, Huazhong University of Science and Technology, Wuhan 430022, P.R. China
E-mail: mozhuoxiong@163.com

Key words: Nogo-66 receptor, Nogo-A, C6 cell line, RNA interference, metastasis

containing 10% fetal bovine serum, as described previously (6). Cells were cultured at 37˚C in an incubator containing 5% CO_2 and 100% humidity. Cells in the mid-log phase were used for experiments.

Immunofluorescence staining. C6 cells were grown on coverslips in 24-well culture plates for 24 h. After fixation for 10 min in 4% formalin or paraformaldehyde, cells were permeabilized with methanol for 2 min at room temperature. After fixation/permeabilization, the slides were rinsed with phosphate-buffered saline (PBS), blocked with 1% bovine serum albumin (BSA) in PBS for 1 h at room temperature or overnight at 4˚C and incubated with primary antibody (1:500; anti-Nogo-66 receptor, Santa Cruz Biotechnology). The cells were washed again with PBS and incubated for 1 h at room temperature with FITC-conjugated secondary antibody (1:200 dilution). Slides were washed and rinsed as described above and then mounted in anti-quenching medium (Sigma, St. Louis, MO, USA). The stained and mounted slides were stored in the dark at 4˚C and fluorescence was visualized with a laser confocal microscope (FV500; Olympus, Tokyo, Japan).

Small hairpin RNA (shRNA) design and transfection. To knock down NgR expression, a vector-based short hairpin RNA (shRNA) expression system was used. The shRNA vector (pGenesil1.1) was purchased from Wuhan Genesil Biotechnology Co., Ltd. The designation of 21 nucleotide target sequences was based on a computer algorithm and 5'-AATCTCACC ATCCTGTGGCTG-3' was selected as the target sequence. The negative control was pGenesil1.1 containing a non-effective scrambled shRNA. For transfection, C6 cells were seeded in 6-well plates to 80% confluency and transfected with 4 μg of plasmid DNA using Lipofectamine 2000 (Invitrogen, Carlsbad, CA, USA). RNA and proteins from scrambled shRNA- or shRNA-transfected cells were analyzed 72 h after transfection.

Detection of NgR mRNA by reverse transcription polymerase chain reaction (RT-PCR). Total RNA extraction and cDNA amplification were performed as described previously (7). The following oligonucleotides were used for RT-PCR analysis: NgR: 5'-AATGAGCCCAAGGTCACAA-3' (sense), 5'-CCATGCAGAAAGAGATGCGT-3' (antisense); β-actin: 5'-GAGAGGGAAATCGTGCGTGAC-3' (sense), 5'-CAT CTGCTGGAAGGTGGACA-3' (antisense). The PCR conditions were as follows: predenaturation at 94˚C for 10 min; denaturation at 94˚C for 50 sec, annealing at 59˚C for 50 sec and extension at 72˚C for 1 min; and a final incubation at 72˚C for 7 min. The amplified products were resolved on 1% agarose by performing homeothermic gel electrophoresis at 80 V for 30 min. The bands were excised and eluted from the gel, purified, precipitated overnight with ethanol and sequenced. The electrophoresis results were observed under an ultraviolet lamp and a density scan of the positive bands was performed. Then, the refractive index (RI) of NgR mRNA was calculated using the formula RI = NgR mRNA density/β-actin density x 100%.

Western blot analysis. Cells were lysed with RIPA buffer, electrophoresed on a 10% SDS-PAGE gel at 100 V for 2 h and electroblotted onto a polyvinylidene fluoride membrane at 275 mA for 2 h. The membrane was incubated with 5% fat-free milk in PBS for 2 h at room temperature. Then, the membrane was incubated in rabbit anti-NgR primary antibody (1:200; Santa Cruz Biotechnology), rabbit anti-cleaved caspase-3 mAb (1:300; Cell Signaling Technology), or mouse anti-β-actin primary antibody (1:1,000; Abcam) overnight at 4˚C. After the membranes were washed with PBS three times, they were incubated in horseradish peroxidase-conjugated anti-rabbit IgG or anti-mouse IgG (1:5,000; Pierce Chemical Co.) for 1 h at room temperature. The samples were washed three times with PBS and developed with an enhanced chemiluminescence reagent (Thermo).

3-[4,5-dimethylthiazol-2-yl]-2,5-diphenyltetrazolium bromide (MTT) assay. The proliferation rates of sh-NgR cells and control cells were measured by an MTT assay. Briefly, NgR-targeted cells or control cells were plated at an initial density of $5x10^3$/well in 96-well plates and incubated for 1, 2, 3, 4 or 5 days in complete culture medium. Twenty microliters of MTT (5 mg/ml) (Sigma) was added and the cells were incubated for 4 h. After the entire medium was discarded, 150 μl of dimethyl sulfoxide was added into each well. The optical density was determined in a microplate reader at 490 nm with subtraction of the baseline reading. Each time-point was repeated six times.

Cell-matrix adhesion assay. The adhesion assay was done as described previously (8). Briefly, a 96-well microtiter plate was coated with Matrigel (50 μl/well) (Vigorous Biotechnology, Beijing, China) for 1 h at 37˚C and then blocked with BSA (10 mg/ml). After being treated with Nogo-66 (15 μg/ml) (Biosynthesis Biotechnology, Beijing, China) or IgG (10 μg/ml) for 2 h at 37˚C, C6 cancer cells were then seeded onto these components. The cells were allowed to adhere to each well for 1 h at 37˚C and were gently washed three times with PBS. The adhesion of C6 cancer cells to the extracellular components was counted at five fields per well at random under a microscope. All experiments were performed in triplicate.

Cell invasion assay. The invasion activity of C6 cancer cells was measured by the previously reported method with some modifications (6). Briefly, C6 cells ($1.25x10^5$ per well) were seeded in the upper chamber separated with an 8-μm membrane filter coated with 15 μg/ml Nogo-66 or IgG (10 μg/ml), which was diluted into extracellular matrix (ECM, Sigma). Medium in the upper chamber was supplemented with 10% fetal bovine ferum (FBS). In the lower chamber, the FBS concentration was 20%. After incubation for 72 h at 37˚C, C6 cells invading the lower chamber were manually counted under a microscope. Six randomly selected fields were counted for each assay. Mean values from six fields were calculated as sample values. For each group, the cell culture was performed in triplicate.

Scratch wound migration assay. C6 cells were grown to confluency in 35-mm wells ($3x10^5$ cells/well). Wounds were scratched using a 200 μl pipette tip and cells were washed three times with PBS. Serum-free DMEM was then added. Triplicate wells were used per condition and three fields per well were captured at each time-point over a period of 24 h. Scratch wound assays were performed for cells from three

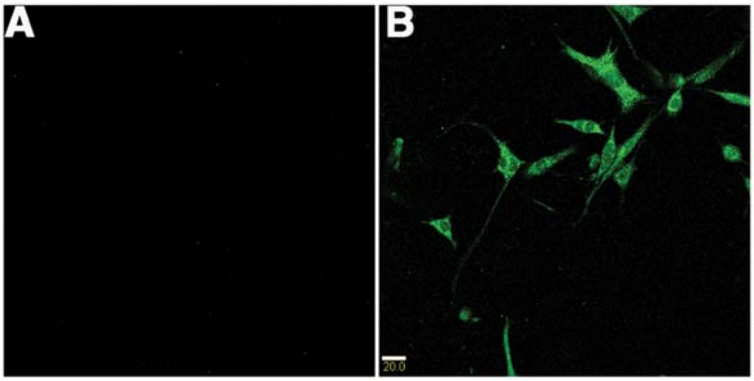

Figure 1. Immunofluorescence analysis of NgR expression in C6 glioma cells. Immunofluorescence and confocal microscopy were used to determine NgR expression on C6 cells. Control images included C6 cells incubated with no primary antibody but with a goat anti-rabbit secondary antibody (A). C6 cells expressing NgR were stained with anti-NgR antibody. As expected, NgR was highly detected by immunofluorescence in the C6 cells (B) (x400 magnification). Scale bar, 20 μm.

independent infections. For experiments in which Nogo-66 was used, confluent monolayers were treated with 15 μg/ml Nogo-66 before wound initiation.

Wounds were visualized using a Nikon Eclipse TS100 microscope (Nikon, Kingston Upon Thames, UK), images were captured using a Coolpix 4500 camera (Nikon) and cells migrating through a central strip were counted in each group.

Flow cytometry of cells. Spontaneous apoptosis of C6 cells was examined by an Annexin V-FITC/propidium iodide (PI) Apoptosis Detection kit (BestBio, China). After shRNA vector was transfected for 48 h, cells were washed with ice-cold PBS and resuspended in 400 μl of 1X binding buffer and the cells were stained with 5 μl of Annexin V and 5 μl of PI for 15 min at 4˚C in the dark. Then, the stained cells were analyzed by fluorescence-activated cell sorting (BD Biosciences, USA) using CellQuest Research Software (BD Biosciences).

Terminal deoxynucleotidyl transferase dUTP nick end labeling (TUNEL) assay. To observe the extent of spontaneous apoptosis, cells were cultured on coverslips in 6-well culture plates. Cells were fixed with 4% formalin for 10 min at 4˚C and then permeabilized with 0.1% Triton-X 100 for 5 min, incubated with reagents from a fluorescein-conjugated TUNEL kit (Roche, Canada) for 1 h at 37˚C and stained with Hoechst 33342 dye (5 μg/ml) for 15 min at room temperature. After washing with PBS, the number of apoptotic cells was visualized by using a laser scanning confocal microscope (FV500; Olympus, Tokyo, Japan) from five random fields.

Statistical analysis. Statistical analysis was performed using Statistical Package for the Social Sciences (SPSS; version 11.5; Bizinsight, Beijing, China). $P<0.05$ was considered statistically significant. Intergroup data were compared using analysis of variance (ANOVA). The quantities of NgR mRNA were consistent with normal distributions and were analyzed using the Student-Newman-Keul's (SNK) test.

Results

NgR is highly expressed in C6 cells. Immunofluorescence was used to identify the presence of NgR in C6 cells. The immunofluorescence experiment was performed with anti-rabbit NgR antibody. As expected, strongly positive cytoplasmic NgR staining was evident in C6 tumor cell lines (Fig. 1).

Downregulation of NgR expression by shRNA in C6 cell lines. RT-PCR analysis was used to detect the changes of NgR mRNA expression after transfection. A 450-bp band was observed in the blank control, the scrambled shRNA group and the NgR shRNA group; and the relative densities of the NgR band compared with the β-actin band were 0.591±0.038, 0.539±0.028 and 0.105±0.009, respectively. There was no significant difference in the density of the NgR mRNA band between the blank control and the scrambled shRNA groups; whereas compared with the blank control, the density of the band in the shRNA group was dramatically less (Fig. 2A and C). Similar to the RT-PCR results, expression of the NgR protein in each group was also observed by western blotting and the relative densities of the NgR band compared with the β-actin band were 0.446±0.059, 0.389±0.085 and 0.162±0.048, respectively (Fig. 2B and D). These data indicate that NgR shRNA can inhibit NgR mRNA and protein expression after transfection into C6 cells.

shRNA against NgR suppressed proliferation of C6 in vitro. Cell proliferation after NgR silencing was assessed by an MTT assay. As shown in Fig. 3, the sh-NgR cells had a lower proliferation rate than the sh-scramble cells. Knockdown of NgR led to a decrease in C6 cell growth at 3 (23.0%), 4 (27.7%) and 5 days (26.1%) ($P<0.05$), compared with the scramble control. These results demonstrate that NgR silencing inhibits the proliferation of C6 cells.

shRNA against NgR enhances cell adhesion of C6 cells in vitro. In the Nogo-66-coated experiment, 1 h after seeding, the number of adherent living cells was significantly increased in the NgR knockdown group compared to the C6 scramble control group (Fig. 4). As a result, the total number of cells increased in the NgR knockdown group. In the IgG-coated experiment, 1 h after seeding, the number of adherent living cells in the NgR knockdown group was not significantly different than that in the C6 control group. These results suggest that NgR knockdown in C6 cells enhances cell adhe-

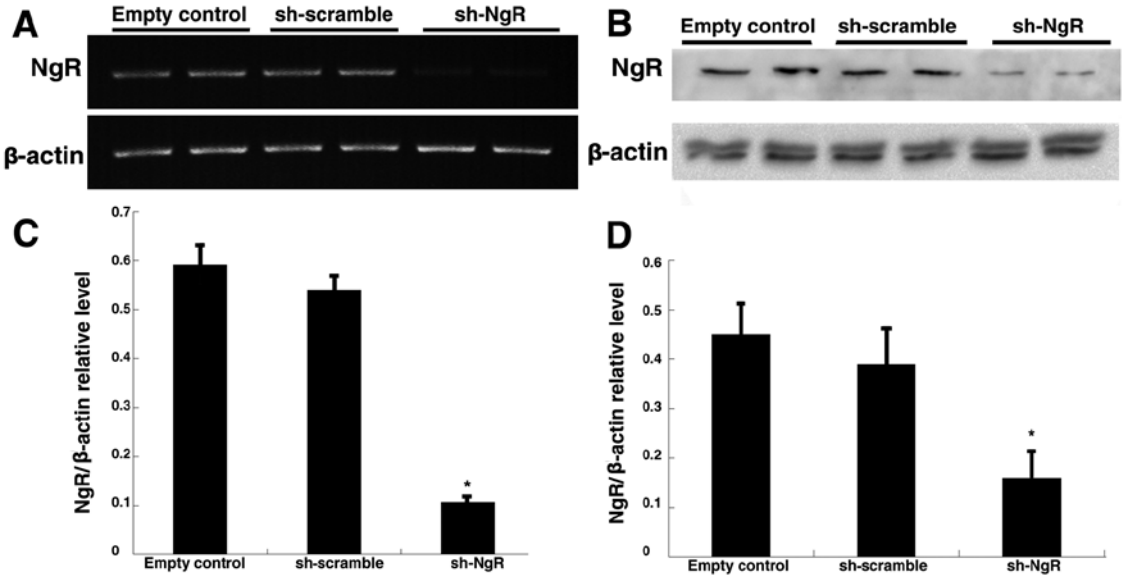

Figure 2. RT-PCR and western blot analyses of NgR expression in C6 cells and C6 cells transfected with shRNA. (A) The expression level of NgR mRNA in the shRNA group was dramatically less compared to the empty vector group or scrambled shRNA group. (B) The protein expression levels of NgR were measured by western blotting. Compared with the empty vector group or scrambled shRNA group, the protein expression level of NgR in the shRNA group was less. Quantitative data of NgR mRNA (C) and protein (D) are shown in the lower panel (*P<0.05, respectively). Data are shown as means ± SD of five experiments.

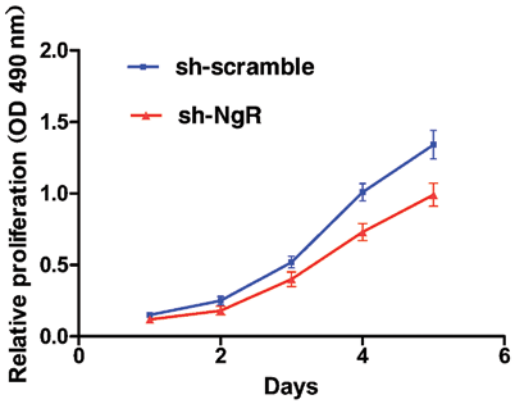

Figure 3. Effect of NgR downregulation on cell proliferation: growth curves of NgR shRNA-targeted cells and scramble control cells were determined by an MTT assay.

sion to Nogo-66-coated Matrigel but does not affect cell adhesion to IgG-coated Matrigel.

shRNA against NgR enhanced cell invasion of C6 cells in vitro. We tested whether NgR knockdown affected the invasion capability of C6 cells by using a Boyden chamber assay. Cells were seeded in the upper part of a Nogo-66/ECM-coated invasion chamber containing a low (10%) FCS concentration. After 72 h, cells that migrated in the lower chamber containing a higher (20%) FCS concentration were stained and counted. In NgR-shRNA C6 cell lines, the number of cells in the membrane was significantly greater than that of the scramble control (Fig. 5). In the IgG/ECM-coated invasion chamber, no further decrease in invasion was observed between NgR-shRNA cells and control cells. These results indicate that invasion through the Nogo-66-coated membrane was significantly enhanced by NgR knockdown in C6 cells but did not affect cell adhesion to the IgG/ECM-coated membrane.

To further test whether NgR knockdown affected the invasion capability of C6 cells, a scratch wound migration assay was used. A wound was scratched in a confluent monolayer of NgR-shRNA cells and scramble control cells coated with Nogo-66 (Fig. 6). The edge of the wound was monitored over 24 h and images of the same fields were taken 0 and 24 h later. The width of the wound in NgR-shRNA C6 cells was significantly narrower than that in the control group. This result indicates that the invasion ability of C6 cells to Nogo-66-coated coverslips was significantly enhanced by NgR knockdown.

shRNA against NgR increased apoptosis of C6 cells in vitro. C6 cells stained with the double stain Annexin V/PI were analyzed by flow cytometry (Fig. 7A and D). The apoptotic rate of C6 cells was 3.21±1.29% in the scramble control group. After NgR knockdown for 48 h, the rate of apoptosis increased to 16.63±0.58%. Thus, the rate of apoptosis in NgR knockdown cells showed a notable increase compared to controls. NgR knockdown in C6 cells significantly increased the expression of caspase-3 (active form) when compared with the scramble control group (Fig. 7B and F). The increased apoptosis rate in NgR knockdown-C6 cells was also evident from the TUNEL-positive staining results (Fig. 6C and E). The rate of TUNEL-positive cells in sh-NgR-C6 cells was 10.21±1.04%, whereas that in the control group was 1.43±0.69%. These results suggest that knockdown of NgR increased the apoptotic rate of C6 cells.

Discussion

Glioma is the most common and aggressive form of the brain tumors. Despite advances in surgical and clinical

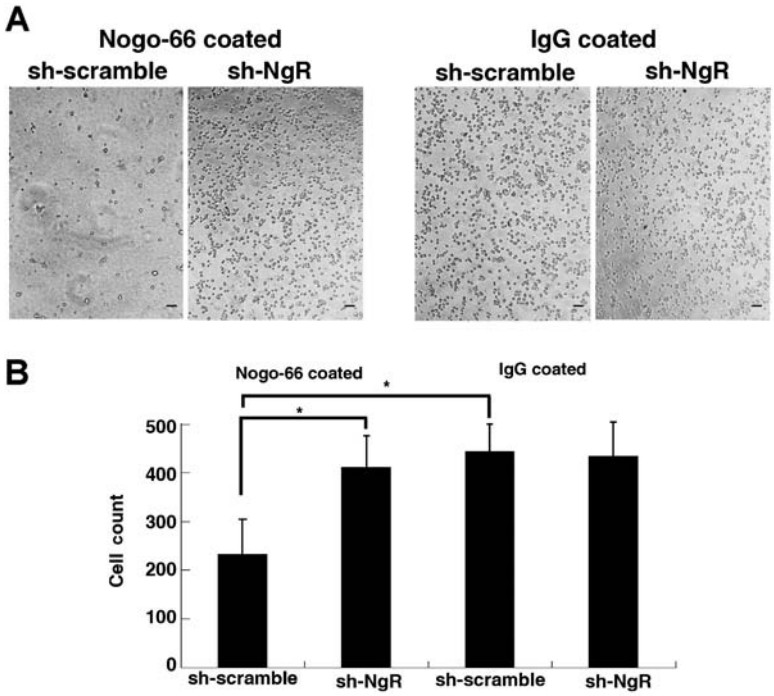

Figure 4. Effect of NgR suppression on cell adhesion. (A) A phase contrast image of C6 cells shows representative cells adhering to the well coated with IgG or Nogo-66 (x100 magnification). Scale bar, 50 μm. (B) Quantification of the effect of NgR downregulation on cell adhesion. In Nogo-66-coated wells, the average number of adherent cells with scrambled shRNA and NgR-shRNA was 228.4±35 and 401.7±62, respectively. In IgG-coated wells, the average number of adherent cells with scrambled shRNA and NgR-shRNA was 429.0±47 and 417.4±58, respectively. Cell adhesion of sh-NgR cells to Nogo-66 was significantly greater compared with parental cells, whereas cell adhesion of sh-NgR cells to Matrigel coated with IgG had no difference compared with parental cells. Data are shown as the means ± SD. *P<0.05.

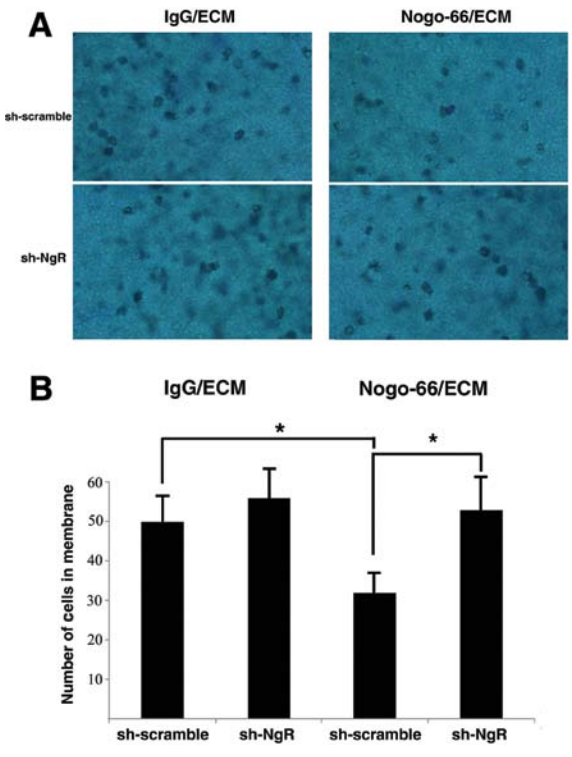

Figure 5. Effect of NgR suppression on cell invasion. (A) Cell invasion through a membrane filter coated with Nogo-66/ECM or IgG/ECM alone was examined. After 72 h, invading cancer cells were stained by hematoxylin and counted under a microscope (x400 magnification). (B) In the Nogo-66/ECM-coated experiment, the number of invading sh-NgR cells was significantly greater than that of untreated cells. In the IgG/ECM-coated experiment, the number of invading sh-NgR cells was not significantly different than that of untreated cells. Data are shown as the means ± SD. *P<0.05.

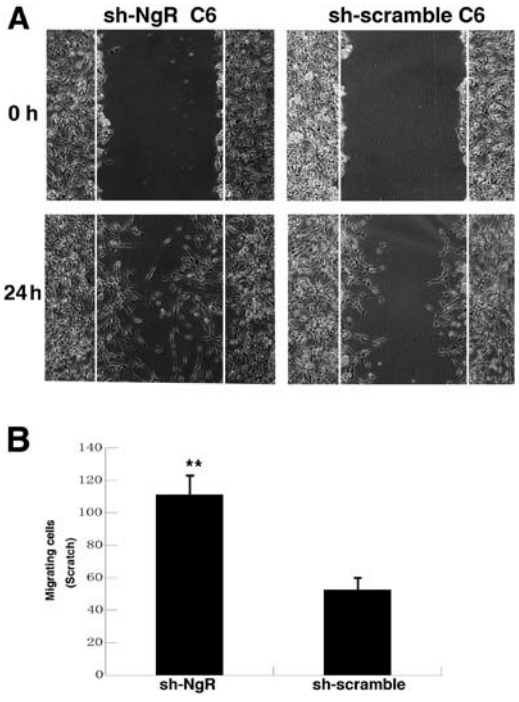

Figure 6. Knockdown of NgR increased the migratory ability of C6 cells as determined by a scratch wound assay. (A) C6 cells were seeded in 24-well plates. After 24 h, a wound was scratched in a confluent monolayer of control and sh-NgR C6 cells. The edge of the wound was monitored over 24 h and images of the same fields were taken at 0 and 24 h (x100 magnification). Scale bars, 50 μm. Representative images from three independent experiments are shown. (B) Quantification of cell migration in (A) was assessed by counting the number of cells in the central gap. The average cell migration of the scrambled shRNA and NgR-shRNA was 54±11 and 112.5±19, respectively. Data are presented as the means ± SD of three independent experiments (**P<0.01).

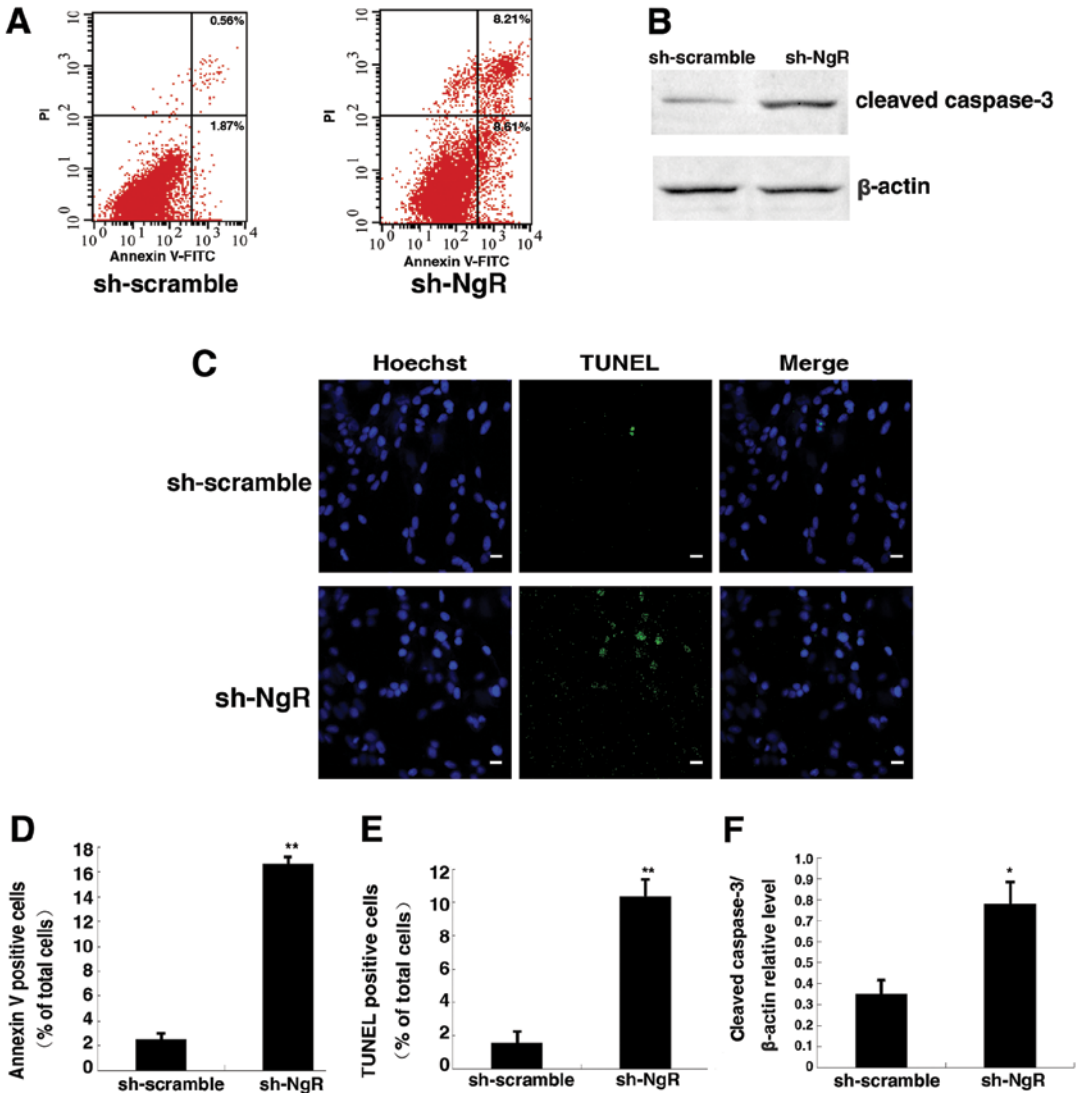

Figure 7. Knockdown of NgR increased apoptosis of C6 cells. (A) Flow cytometric analysis of apoptosis in C6 cells. The upper right quadrant (UR) represents the percentage of early apoptotic cells and the lower right quadrant (LR) represents the percentage of late apoptotic cells. (B) The expression levels of cleaved-caspase-3 were detected by western blot analysis. (C) DNA fragmentation was observed using TUNEL staining. Images of nuclei stained with Hoechst 33342 and the TUNEL kit are shown (x400 magnification). Scale bar, 20 μm. (D) Quantification of annexin-positive cells is shown. **P<0.01 versus the scrambled control group. (E) The percentage of TUNEL-positive cells. (F) Quantitation of the relative level of cleaved caspase-3/β-actin depicted in Fig. 6B. Data are shown as the means ± SD of five experiments (*P<0.05; **P<0.01).

neuro-oncology, malignant glioma prognosis remains poor due to its diffusive and invasive nature (9). A key contributor to the pathology of brain tumors is their ability to diffusely infiltrate the parenchyma. Surgical excision of a malignant brain neoplasm is not sufficient to eliminate neoplastic cells that have infiltrated normal adjacent brain. Therefore, it is of primary importance to determine the mechanisms involved in brain tumor cell adhesion and invasion (10).

The invasion of glioma cells depends upon multiple factors, including ECM molecules, growth factors and the activity of intracellular pathways regulating cell motility (11). The brain ECM, composed of cytotactin/tenascin-C, laminin, thrombospondin, vitronectin and fibronectin, is synthesized and secreted by astrocytes during development and is involved in adhesion and migration of neurons and glia during development (12,13). *In vitro* studies using glioma cell lines indicate that brain tumor cells can use some of these ECM molecules as favorable substrates for migration (14,15).

We previously investigated the expression of NgR protein in human astrocytoma (4). The results showed that the expression of NgR protein markedly decreased with increasing pathological grades. Double immunostaining results showed that Nogo-A and NgR were colocalized on the surface of tumor cells in astrocytoma tissues. Our results confirmed that the distribution of Nogo-A and NgR at the interface of the tumor cells was negatively related to tumor malignancy and supported the hypothesis that Nogo-A restricts migration of tumor cells. Therefore, NgR may have inhibitory effects on tumor activity and may also be an attractive therapeutic target for human astrocytic tumors.

In the present study, we studied the possible roles of Nogo-66 and NgR in tumor cell migration *in vitro*. Immunofluorescence studies showed the presence of NgR in C6 cells. Our results revealed that NgR-deficient cells had an increased ability of adhesion and invasion in the presence of Nogo-66, whereas there were no changes of adhesion and invasion without

Nogo-66. The data suggest that Nogo-A acts as a negative regulator or 'brake' for C6 tumor cells. In addition, this effect may be mediated by extracellular Nogo-66 via its receptor NgR. A similar result was obtained by Amberger *et al*, who found that low-grade glioma cell lines as well as primary cultures were strongly sensitive to the inhibitory proteins present in CNS myelin (16). In contrast, high-grade glioma cell lines were able to spread and migrate on CNS myelin-coated culture dishes, demonstrating that within the gliomas, the ability to overcome the inhibitory effects of CNS myelin is correlated with the grade of malignancy of the original tumor. These results suggest that myelin was involved in the process of invasive migration of malignant gliomas along CNS white matter fiber tracts.

The nerve tract in the tumor area usually cannot be eroded and discontinued even though the tract is severely compressed by a large tumor entity. The reason why the tract is seldom eroded is not known. The results that myelin molecules in the nerve tract had the ability to inhibit tumor invasion can explain this phenomenon.

Various studies have shown that the poor prognosis of tumors is not only due to over invasion and metastasis but also due to the loss of natural apoptosis (17). Apoptosis is also a crucial mechanism for the control of cell proliferation and increased apoptosis results in glioma cells that are sensitive to chemotherapy and radiation therapy (18). Our data suggest that the downregulation of NgR can decrease the proliferation of C6 cells. Cell apoptosis measured by flow cytometry and TUNEL assays showed that NgR-deficient cells increased the apoptosis of C6 cells. Apoptotic changes in morphology such as the increased ratio of chromatin accumulation, nuclear condensation and DNA fragmentation were also observed in the present study. In corroboration with these results, shNgR treatment resulted in the elevation of cleaved caspase-3 in C6 cells. Silencing of NgR increased the spontaneous apoptosis of C6 cells 3-fold, compared to control cells. Kilic *et al* found that Nogo-A and its receptor blockade led to decreased neuronal survival (5). Our results were similar to the report by Kilic *et al*. However, the detailed mechanism regarding the effect of NgR knockdown on cell apoptosis was not investigated and there has been no research describing the effect of NgR knockdown on spontaneous apoptosis in glioma cells.

Apoptosis typically involves a series of events that are associated with Bcl-2 family members regulating mitochondrial release of cytochrome *c* and activation of a cascade of caspases and various endoplasmic reticulum stresses, finally leading to the fragmentation of chromosomal DNA (19,20). In addition, apoptosis is directly modulated by different members of the Ras and Rho GTPase superfamilies. Furthermore, Kilic *et al* evaluated injured neuronal cells by a TUNEL assay and showed that Nogo-A blockade decreased neuronal survival through deactivation of the small GTPases RhoA, Rac1 and RhoB (5). NgR in glioma cells might act as a tumor apoptosis inhibitor via RhoA deactivation. In the future, we will undertake in-depth research to confirm our hypothesis.

Recently, it has been reported that Nogo-66 inhibits adhesion and migration of microglia via RhoA activation and Cdc42 deactivation, but the signal transduction pathways involved in RhoA triggered by Nogo-66/NgR require more detailed research (21).

In conclusion, we found that Nogo-66 and NgR have been well-studied for their inhibitory functions on axon growth in the adult CNS and play a role in the regulation of tumor C6 cell migration, invasion and apoptosis *in vitro*. However, many mechanistic details remain to be studied. For example, whether the effects of Nogo-66 and NgR on migration are mediated through a receptor complex that includes Lingo-1 and p75 remains to be determined. In particular, whether Rho-A is involved in the signaling pathway downstream of NgR is not known. The precise mechanism of NgR knockdown on the effect of apoptosis in tumor cells also remains to be elucidated.

Acknowledgements

This study was supported by research grants from the National Nature Science Foundation of China (30471775, 30801180) and the Hubei Research Development Project Foundation (2005AA301C15).

References

1. Chen MS, Huber AB, van der Haar ME, Frank M, Schnell L, Spillmann AA, Christ F and Schwab ME: Nogo-A is a myelin-associated neurite outgrowth inhibitor and an antigen for monoclonal antibody IN-1. Nature 403: 434-439, 2000.
2. Fournier AE, GrandPre T and Strittmatter SM: Identification of a receptor mediating Nogo-66 inhibition of axonal regeneration. Nature 409: 341-346, 2001.
3. Liao H, Duka T, Teng FY, Sun L, Bu WY, Ahmed S, Tang BL and Xiao ZC: Nogo-66 and myelin-associated glycoprotein (MAG) inhibit the adhesion and migration of Nogo-66 receptor expressing human glioma cells. J Neurochem 90: 1156-1162, 2004.
4. Xiong N, Shen J, Li S, Li J and Zhao H: Expression of Nogo-66 receptor in human astrocytoma is correlated with tumor malignancy. Mol Biol Rep 39: 2625-2632, 2012.
5. Kilic E, ElAli A, Kilic U, Guo Z, Ugur M, Uslu U, Bassetti CL, Schwab ME and Hermann DM: Role of Nogo-A in neuronal survival in the reperfused ischemic brain. J Cereb Blood Flow Metab 30: 969-984, 2010.
6. Albini A, Iwamoto Y, Kleinman HK, Martin GR, Aaronson SA, Kozlowski JM and McEwan RN: A rapid in vitro assay for quantitating the invasive potential of tumor cells. Cancer Res 47: 3239-3245, 1987.
7. Kawajiri H, Yashiro M, Shinto O, Nakamura K, Tendo M, Takemura S, Node M, Hamashima Y, Kajimoto T, Sawada T, *et al*: A novel transforming growth factor beta receptor kinase inhibitor, A-77, prevents the peritoneal dissemination of scirrhous gastric carcinoma. Clin Cancer Res 14: 2850-2860, 2008.
8. Nishimura S, Chung YS, Yashiro M, Inoue T and Sowa M: Role of alpha 2 beta 1- and alpha 3 beta 1-integrin in the peritoneal implantation of scirrhous gastric carcinoma. Br J Cancer 74: 1406-1412, 1996.
9. Dasari VR, Velpula KK, Kaur K, Fassett D, Klopfenstein JD, Dinh DH, Gujrati M and Rao JS: Cord blood stem cell-mediated induction of apoptosis in glioma downregulates X-linked inhibitor of apoptosis protein (XIAP). PLoS One 5: e11813, 2010.
10. Friedlander DR, Zagzag D, Shiff B, Cohen H, Allen JC, Kelly PJ and Grumet M: Migration of brain tumor cells on extracellular matrix proteins in vitro correlates with tumor type and grade and involves alphaV and beta1 integrins. Cancer Res 56: 1939-1947, 1996.
11. Yang HW, Menon LG, Black PM, Carroll RS and Johnson MD: SNAI2/Slug promotes growth and invasion in human gliomas. BMC Cancer 10: 301, 2010.
12. Eroglu C: The role of astrocyte-secreted matricellular proteins in central nervous system development and function. J Cell Commun Signal 3: 167-176, 2009.
13. Irintchev A, Rollenhagen A, Troncoso E, Kiss JZ and Schachner M: Structural and functional aberrations in the cerebral cortex of tenascin-C deficient mice. Cereb Cortex 15: 950-962, 2005.

14. Giese A, Loo MA, Rief MD, Tran N and Berens ME: Substrates for astrocytoma invasion. Neurosurgery 37: 294-302, 1995.
15. Giese A, Rief MD, Loo MA and Berens ME: Determinants of human astrocytoma migration. Cancer Res 54: 3897-3904, 1994.
16. Amberger VR, Hensel T, Ogata N and Schwab ME: Spreading and migration of human glioma and rat C6 cells on central nervous system myelin in vitro is correlated with tumor malignancy and involves a metalloproteolytic activity. Cancer Res 58: 149-158, 1998.
17. Matsushita S, Nitanda T, Furukawa T, Sumizawa T, Tani A, Nishimoto K, Akiba S, Miyadera K, Fukushima M, Yamada Y, *et al*: The effect of a thymidine phosphorylase inhibitor on angiogenesis and apoptosis in tumors. Cancer Res 59: 1911-1916, 1999.
18. Ghobrial IM, Witzig TE and Adjei AA: Targeting apoptosis pathways in cancer therapy. CA Cancer J Clin 55: 178-194, 2005.
19. Rossi L, De Martino A, Marchese E, Piccirilli S, Rotilio G and Ciriolo MR: Neurodegeneration in the animal model of Menkes' disease involves Bcl-2-linked apoptosis. Neuroscience 103: 181-188, 2001.
20. Hengartner MO: The biochemistry of apoptosis. Nature 407: 770-776, 2000.
21. Yan J, Zhou X, Guo JJ, Mao L, Wang YJ, Sun J, Sun LX, Zhang LY, Zhou XF and Liao H: Nogo-66 inhibits adhesion and migration of microglia via GTPase Rho pathway in vitro. J Neurochem 120: 721-731, 2012.